

# A MULTICHANNELLED BACTERIAL CELLULOSE SCAFFOLD FOR 3D IN VITRO CANCER CULTURE

HONGLIN LUO,\* FENG GU,\*\* GUANGYAO XIONG,\*\* DA HU,\*\*  
YONG ZHU\*\*\*\* and YIZAO WAN\*\*\*\*

\**Institute for Biomaterials and Transportation, East China Jiaotong University,  
Nanchang 330013, Jiangxi, China*

\*\**Department of Breast Pathology, Tianjin Medical University Cancer Institute and Hospital, Key  
Laboratory of Breast Cancer Prevention and Therapy of the Ministry of Education, Key Laboratory of  
Cancer Prevention and Therapy of Tianjin, China*

\*\*\**School of Mechanical and Electrical Engineering, East China Jiaotong University,  
Nanchang 330013, Jiangxi, China*

\*\*\*\**School of Materials Science and Engineering, Tianjin University, Tianjin 300072, China*

\*\*\*\*\**School of Chemical Engineering, Tianjin University, Tianjin 300072, China*

✉ *Corresponding author: Yizao Wan, yzwantju@126.com*

Received May 22, 2014

Artificial three-dimensional (3D) *in vitro* tumor models mimicking the native cell architecture and environments are highly desirable tools for studying tumor progression and screening therapeutics. In this work, a 3D bacterial cellulose (BC) scaffold with multichanneled macropores (~300  $\mu\text{m}$ ) was fabricated. The obtained MM-BC scaffold was characterized by SEM, mercury intrusion porosimeter, contact angle and mechanical measurements, and determined for its potential as a tumor model. It was demonstrated that the MM-BC scaffold exhibited hierarchical pore structure and sufficient mechanical strength. Moreover, the MM-BC scaffold supported the adhesion, migration, and proliferation of primary culture cancer cells, allowed the cells' infiltration into the core of the scaffold. The results suggested that the MM-BC scaffold can be an effective *in vitro* tumor model to study cancer progression and drug screening.

**Keywords:** bacterial cellulose, multichannel, pore structure, tumor model, cancer cell

## INTRODUCTION

It has been well accepted that a scaffold with *in vivo* architecture and *in vivo* environments should be employed in order to design and fabricate a biological tissue or organ with natural functions. To this end, three-dimensional (3D) scaffolds should be employed in both tissue engineering and tumor engineering (which, according to Ghajar and Bissell, is the construction of complex cell culture models that recapitulate aspects of the *in vivo* tumor microenvironment to study the dynamics of tumor development, progression, and therapy on multiple scales<sup>1</sup>) from a biomimetics point of view because tissues and organs are 3D.<sup>2</sup> Nevertheless, our understanding on the formation, function, and pathology are mainly from two-dimensional (2D) cell culture studies or animal model systems. A growing number of studies have recognized that

cancer cells cultured in 2D cannot accurately represent their *in vivo* physiological conditions.<sup>2-5</sup> On the other hand, animal models may not adequately reproduce features of human tumors, drug therapeutic responses, autoimmune diseases, and stem cell differentiation.<sup>2</sup> Therefore, *in vitro* 3D tumor models are believed to be a third approach that bridges the gap between traditional 2D cell culture and animal models.<sup>2,6</sup> In this context, 3D scaffolds have begun their applications in cancer research where the goal is to accurately understand tumor progression, metastasis and provide a tool for screening therapeutics *in vitro*.<sup>7</sup> To date, many 3D culture systems have been developed for cancer research and anticancer drug tests.<sup>8-10</sup> Naturally derived matrix materials like Matrigel and collagen have been widely used and

significant findings related to tumor phogenesis and matrix invasion in a 3D environment have been gained.<sup>11</sup> Meanwhile, more materials are being explored. In addition, researchers are also turning to the modulation of physical nature of scaffolds such as fiber diameter and pore size and shape.<sup>12,13</sup> For instance, a recent study demonstrated that the acrylate copolymer-based scaffolds with aligned channels of pore diameters in the range from 40 to 80  $\mu\text{m}$  achieved uniform colonization by neural cells.<sup>14</sup> However, the pores were small in diameter and cell infiltration into the bulk space was not demonstrated.<sup>12,13</sup> To the best of the authors' knowledge, there is no report regarding the influence of macropore (larger than 100  $\mu\text{m}$  in diameter according to the literature<sup>15,16</sup>) on tumor cells behavior, although it has been well documented that the pore diameter in the scaffolds for tissue engineering is generally ranged between 100 and 800  $\mu\text{m}$ .<sup>17</sup> In addition, pore structure is also an important parameter affecting cells' behavior. In tissue engineering, pore structure (including pore shape, porosity, and interconnectivity) is believed to determine cell in-growth and proliferation within the scaffolds, and integration with surrounding tissues.<sup>18,19</sup> Interestingly, in tumor engineering, a pioneer work by Szot and co-workers has demonstrated that cancer cells cultured on bacterial cellulose (BC) exhibited decreased proliferation, viability, and an abnormal morphology due to the lack of macropores and low porosity.<sup>20</sup> This pioneer study indicates the direction of research on designing tumor models with BC. It is reasonable to hypothesize that pore structure may also affect the interaction between tumor cells and scaffolds. To test this hypothesis, a new 3D *in vitro* tumor model with multichanneled macropores was fabricated by using a nanofibrous BC material.

BC is synthesized extracellularly by the bacterium *Acetobacter xylinum*. In addition to such appealing properties as ultrahigh mechanical strength and modulus, high water holding capability and porosity, and good biocompatibility,<sup>21,22</sup> BC displays intrinsic 3D network structure, and, in particular, BC fibers are in the nanometer scale, which is the low limit of natural ECM fibers. BC has received enormous research interest in the field of tissue engineering over recent years.<sup>23,24</sup> However, some drawbacks impede the usage of BC in the biomedical field. One of the biggest problems of BC is the absence of macropores within BC scaffolds.<sup>25</sup>

Therefore, in this work, a BC scaffold with multichanneled macropores (denoted as MM-BC) was developed in an attempt to find a new tumor model for cancer research and drug evaluation. The purpose of the present study was to prepare a MM-BC scaffold, and then to examine its morphology and mechanical properties, and to preliminarily determine the feasibility of this scaffold as an effective *in vitro* tumor model. To this end, primary culture cancer cells were cultured on this BC scaffold to investigate the behavior of cancer cells.

## EXPERIMENTAL

### Preparation of MM-BC scaffold

The preparation procedure of BC pellicles was described in our previous work.<sup>26-28</sup> Briefly, the bacterial strain, *Acetobacter xylinum* X-2, was grown in the culture media containing 0.3 wt% green tea powder (analytical grade) and 5 wt% sucrose (analytical grade) for 7 days. The pH of the medium was adjusted to 4.5 by acetic acid. BC pellicles were purified by soaking in deionized water at 90 °C for 2 h followed by boiling in a 0.5 M NaOH solution for 15 min. The pellicles were then washed with deionized water for several times and soaked in 1 wt% NaOH for 2 days. After rinsing with deionized water until neutral pH, the BC pellicles were taken out for the creation of macropores. The multichanneled pores were fabricated by a laser-aided punching process. Typically, the pore pattern (including distance between neighboring pores and pore diameter) was initially designed by a commercial CAD software and input to a computer. The BC hydrogels were then punched using a CO<sub>2</sub> excimer laser (wavelength 10.6  $\mu\text{m}$ ) according to the designed pattern. In this work, the designed pore size and pore distance were 300  $\mu\text{m}$  and 1 mm, respectively.

### Field emission scanning electron microscopy (FE-SEM)

The morphology of the MM-BC scaffold was observed by using a Nano 430 field emission scanning electron microscope (FE-SEM), FEI, USA. For FE-SEM observation, samples were sputter coated with gold and were observed at an accelerating voltage of 10 kV.

### Mercury porosimeter

The pore size distribution of the MM-BC scaffold was determined by a PoreMaster 60 GT mercury intrusion porosimeter (Quantachrome) that was designed to measure pore diameter ranging from 950  $\mu\text{m}$  to up to 3.6 nm.

### Contact angle measurement

Contact angle measurement was conducted on a

contact angle goniometer (Kyowa Interface Science, Master 300) using deionized water as medium at room temperature. All contact angles were determined by averaging the values measured at three different points on each sample's surface. The drop images were taken with a high-resolution IIEEE1394 camera.

### Mechanical testing

Similar to the process reported earlier,<sup>29</sup> the tensile properties of MM-BC and pristine BC samples in wet state were determined in accordance with ASTM D 638-98 Type IV specimens using a Testometric universal testing machine M350 (Testometric Co. Ltd., United Kingdom). The measurement was performed with a constant crosshead speed of 1 mm/min under ambient temperature and a humidity of 45% RH. The tensile strength was determined as the maximum point of the force-strain curve and the average values were calculated from at least five separate tests.

### Cell studies

#### MTT proliferation assay

The cell proliferation on the MM-BC scaffold was quantitatively determined using the colorimetric MTT assay. The primary culture cancer cells were maintained in DMEM (Gibco) with 10% FBS (Gibco) at 37 °C in a 5% CO<sub>2</sub> incubator. The culture medium was changed every two days. Monolayer cells were harvested by trypsin/EDTA treatment. Before cell seeding, a circular BC scaffold (Φ5 × 3 mm) was sterilized with UV radiation, followed by pre-soaking in DMEM for at least 12 h. The sterilized MM-BC scaffold was placed into 24-well culture plates and seeded with a cell suspension with a cell density of 2×10<sup>5</sup> cells/ml, followed by culturing for 1, 3, 5, 7 days at 37 °C in a 5% CO<sub>2</sub> incubator. After incubation, the cell-scaffold constructs were rinsed with PBS, followed by incubation in 50 μL MTT reagent for 4 h. After removal of the media, 500 μL of DMSO was added to the wells. The solution (150 μL) from each sample was transferred to 96-well plates and the absorbance of the solution was measured at a wavelength of 490 nm.

#### Cell imaging

The morphology of the cells on the MM-BC scaffold was observed by the same scanning electron microscope as described above. After pre-soaking with DMEM overnight, the MM-BC scaffold was incubated with the cells at a density of 2×10<sup>5</sup> cell/mL in 24-well plates for 7 days at 37 °C in 5% CO<sub>2</sub>. After incubation, the cell-scaffold samples were rinsed twice with PBS and fixed using 4% glutaraldehyde for 12 h, and then dehydrated through gradient concentration of alcohols (40%, 50%, 60%, 70%, 80%, 90% and 100%), and air-dried. Finally, the samples were sputter-coated with a layer of gold and observed by SEM.

### Histological analysis

After 1, 2, and 3 weeks of culture, the cell-scaffold constructs were washed with ice-cold normal saline (0.9% NaCl), cut transversely into thin slices (5 μm), and then fixed into 10% neutral-buffered formaldehyde for 24 h. The samples were then transferred into 70% ethanol, processed, paraffin embedded and hematoxylin and eosin (H&E) stained using standard protocols. The sections with cells were examined using a Zeiss Axioplan-2 fluorescence light microscope (Carl Zeiss, Inc., NY).

### Statistical analysis

All experiments were performed in triplicate unless otherwise stated. Statistical analysis of the data was performed using an SPSS system. All data were presented as mean value ± standard deviation (SD). Results with *p*-values of < 0.05 were considered statistically significant.

## RESULTS AND DISCUSSION

### Morphology of MM-BC scaffold

The photograph and SEM images of the MM-BC scaffold are shown in Fig. 1. As shown in Fig. 1a, a symmetrical pore pattern was formed in the MM-BC scaffold. Measurement under SEM revealed that the pore size was 300 ± 22 μm and the distance between neighboring pores was 1 ± 0.01 mm, which were close to the designed parameters. Fig. 1b and c revealed that the edge of each pore was smooth without obvious debris, which was often observed for UV and femtosecond laser micromachining. Fig. 1d demonstrated that the wall of the macropores was porous, consisting of nanofibers and small pores. The porous wall was believed to enhance cell functions<sup>30</sup> as compared to compact pore wall that hindered metabolite diffusion and restricted cell proliferation and migration inside 3D scaffolds.<sup>31</sup> It was proposed that, when cells were seeded onto the internal porous matrix of the scaffold, the inner porous wall was believed to be able to keep deeply embedded cells supplied with nutrients.<sup>32</sup>

### Pore structure

Fig. 2 displays the pore size distribution of the MM-BC scaffold obtained from mercury intrusion porosimeter measurement. Note that the obtained MM-BC scaffold exhibited hierarchical pore structure since it contained macropores (>100 μm as defined in the literature<sup>15,16</sup>), micropores (<100 μm), and nanopores (<1 μm). This unique pore structure was significantly different from that of the pristine BC scaffold that contained only micropores

and nanopores.<sup>25</sup> In addition, the diameter of the dominant pores in the pristine BC was around 10  $\mu\text{m}$ ,<sup>25</sup> while the MM-BC scaffold exhibited a

dominant pore size of almost 100  $\mu\text{m}$  and the largest pore diameter reached 320  $\mu\text{m}$ , consistent with SEM measurement.

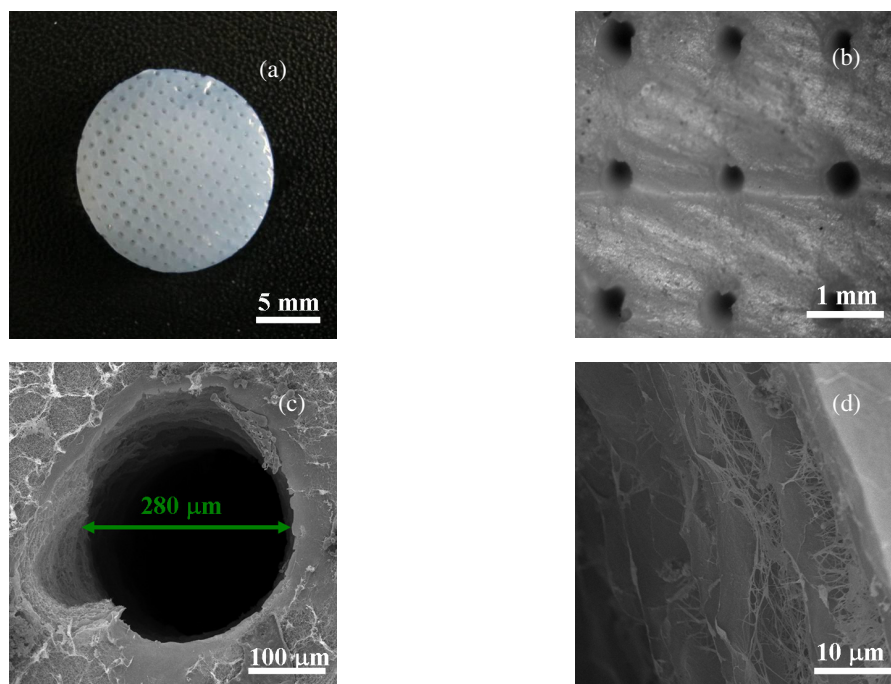


Figure 1: Typical photo (a) and SEM images of the surface (b and c) and pore wall (d) of MM-BC scaffold

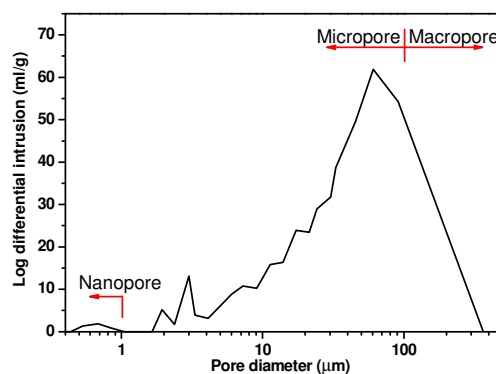


Figure 2: Pore size distribution of MM-BC scaffold

Numerous studies have confirmed that hierarchical porous materials are of increasing importance because of their potential application in bioengineering as well as in catalysis and separation technology.<sup>33</sup> A hierarchical porous scaffold with macropores is of vital importance since a pore diameter larger than 100  $\mu\text{m}$  is recommended in tissue engineering.<sup>17</sup> The scaffold with macropores is of particular interest in tumor

engineering since cancer cells are often larger than normal cells and thus larger space is needed for the migration and infiltration of cancer cells into the inner of a scaffold as compared to normal cells.

#### Water contact angle

The contact angle measurement showed that both MM-BC and pristine BC were hydrophilic (Fig. 3) with a water contact angle of  $49.9 \pm 2.4^\circ$

and  $38.9 \pm 1.9^\circ$ , respectively. The increased contact angle suggested that the presence of macropores significantly increased the surface hydrophilicity. The increase in surface hydrophilicity after punching was not due to the change in the surface free energy since laser punching did not change the chemistry of BC; instead it was due to the presence of macropores that facilitated water infiltration into the inner part of the scaffold and thus resulting in a lower contact angle.

### Mechanical properties

Fig. 4 shows typical stress–strain curves of the MM-BC and pristine BC and the values of tensile strength and modulus and strain at break are listed in Table 1. Note that two scaffolds exhibited a similar stress–strain pattern, showing an initial approximate linear stress increase with respect to the strain, then an obvious yield, and finally a failure. As expected, the MM-BC showed significantly lower tensile strength and modulus ( $p < 0.05$  in both cases) than the pristine BC. This is simply due to the existence of macropores in the

MM-BC, which reduced the effective cross-sectional area. The tensile strength value ( $0.47 \pm 0.01$  MPa) of the MM-BC was still strong enough when compared to other relevant scaffolds such as 2,3-dialdehyde bacterial cellulose ( $0.27 \pm 0.03$ ).<sup>34</sup> Furthermore, as shown in Table 1, the strain at break of the MM-BC was also lower than that of the pristine BC ( $p < 0.05$ ).

### MTT

The MTT results shown in Fig. 5 demonstrated that primary culture cancer cells were viable and proliferated well by keeping almost a linear growth during 7 days of culture, suggesting that the MM-BC scaffold could support the highly invasive metastatic phenotype of cancer cells. However, limited viability and proliferation were reported by Szot *et al.* when cancer cells were cultured on the pristine BC without macropores.<sup>20</sup> The difference in cell proliferation suggested that the pore structure and size of the tumor engineering scaffolds were crucial to the culture of cancer cells.

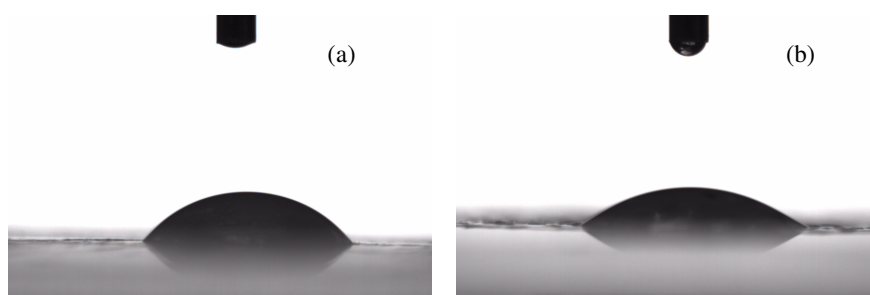


Figure 3: Surface wettability of MM-BC (a) and pristine BC (b)

Table 1  
Tensile strength and modulus and strain at break values for MM-BC and pristine BC

Samples	Tensile strength (MPa)	Tensile modulus (MPa)	Strain at break (%)
BC	$0.77 \pm 0.13$	$20.8 \pm 0.8$	$6.0 \pm 0.8$
MM-BC	$0.47 \pm 0.01$	$13.5 \pm 0.1$	$5.1 \pm 0.4$

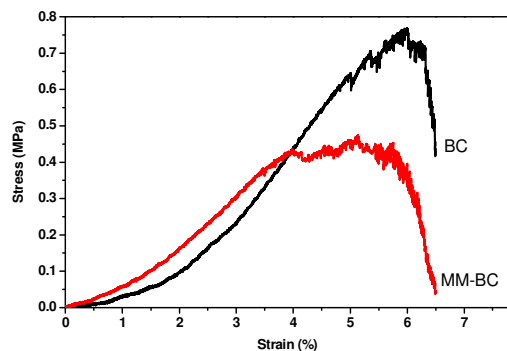


Figure 4: Typical stress–strain curves for MM-BC and pristine BC

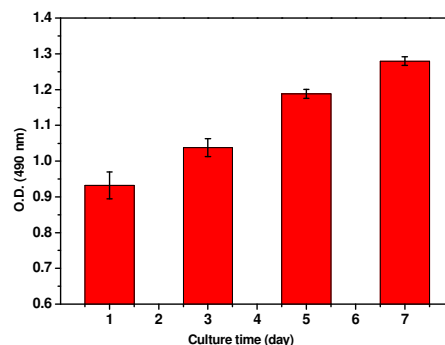


Figure 5: Proliferation of primary culture cancer cells cultured on MM-BC scaffold

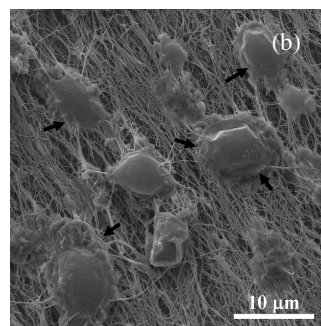
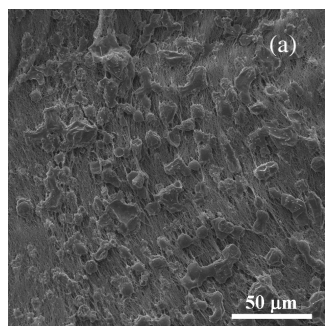


Figure 6: Morphology of primary culture cancer cells cultured on MM-BC scaffold

### Cell morphology

Fig. 6 shows the morphology of primary culture cancer cells 7 days after seeding on the MM-BC scaffold. Note that the cells exhibited vigorous growth and good attachment to the MM-BC scaffold (Fig. 6a). Furthermore, the growing cells on the MM-BC scaffold demonstrated normal cell morphology of roughly rounded shape. Notably, some protruded pseudopodia were formed, which bonded to the scaffold (see arrows in Fig. 6b). This finding indicated a strong adhesion of cancer cells to the scaffold, suggesting that this MM-BC scaffold could support the attachment and spreading of the cancer cells. However, a previous study by Szot *et al.* demonstrated that cancer cells cultured on BC did not spread out across the surface of BC scaffolds due to the absence of manufactured porosity.<sup>20</sup> It is therefore reasonable to conclude that macropores in the MM-BC scaffold played a decisive role in favoring cells' function.

### Histological observation

In order to evaluate the distribution of cells

inside the MM-BC scaffold, histological observation was performed and the results are shown in Fig. 7. As clearly indicated in Fig. 7a, cells were distributed within the macroporous MM-BC scaffold and formed clusters in some areas (circles in Fig. 7), suggesting the infiltration of cancer cells into the scaffold, differing from what was reported in the literature<sup>20</sup>. Furthermore, as indicated by arrows in Fig. 7a and b, the cells spread and grew along the walls of the macropores. Fig. 7b and c showed increased cell density and increased number of clusters (Fig. 7b) around the walls of the macropores over culture time. These results indicated that cancer cells could penetrate into the core of the MM-BC scaffold due to the presence of multichanneled macropores. A similar result was reported by Chrobak *et al.*, who declared that endothelial cells proliferated to confluence along the microchannel wall and dynamically regulated diffusion of fluorescent molecules across the microchannel wall.<sup>35</sup> However, how the porous wall affects the functions of cancer cells, which are larger than endothelial cells, is still unclear and this will be the focus of our future work.

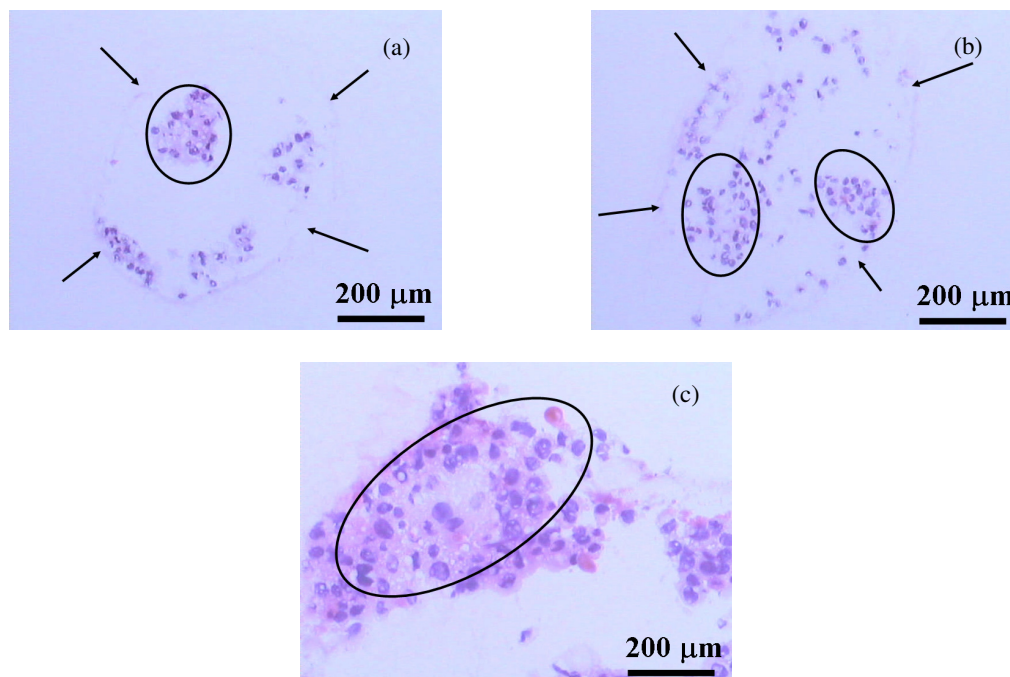


Figure 7: Histological evaluation of primary culture cancer cells after 1 (a), 2 (b), and 3 (c) weeks culture in MM-BC scaffold (arrows indicate the walls of macropores)

Results from MTT, SEM, and histological observation confirm that the BC scaffold with macropores is able to support the adhesion, in-growth, proliferation, and differentiation of cancer cells. Although further deep studies such as gene expression are still in progress, this multichanneled BC scaffold shows promise as a novel scaffold for the *in vitro* culture of cancer cells.

## CONCLUSION

A 3D bacterial cellulose (BC) scaffold with multichanneled macropores (MM-BC) has been created by a laser punching technique. The MM-BC scaffold possessed a hierarchical pore structure with macro-, micro-, and nano-pores, while maintaining a high tensile strength. In addition, the wall of the macropores was porous. MTT results demonstrated that the primary culture cancer cells were viable and proliferated well by keeping a rough linear growth during 7 days of culture. More importantly, MTT, SEM, and histological observation indicate that the MM-BC scaffold with macropores is able to support the adhesion, in-growth, proliferation, and differentiation of cancer cells. A comparison between the current findings with previous results from the pristine BC verifies that the presence of multichanneled

macropores plays a crucial role in favoring cell functions. Thus, this BC-based 3D culture system may provide a new platform for cancer biology study.

**ACKNOWLEDGEMENTS:** This work is supported by the National Natural Science Foundation of China (Grant Nos. 51172158 and 81200663) and the Science and Technology Support Program of Tianjin (Grant No. 11ZCKFSY01700).

## REFERENCES

- <sup>1</sup> C. M. Ghajar and M. J. Bissell, *Tissue Eng. A*, **16**, 2153 (2010).
- <sup>2</sup> K. M. Yamada and E. Cukierman, *Cell*, **130**, 601 (2007).
- <sup>3</sup> M. A. Cichon, V. G. Gainullin, Y. Zhang and D. C. Radisky, *Integr. Biol.*, **4**, 440 (2012).
- <sup>4</sup> G. Y. Lee, P. A. Kenny, E. H. Lee and M. J. Bissell, *Nat. Methods*, **4**, 359 (2007).
- <sup>5</sup> C. Fischbach, R. Chen, T. Matsumoto, T. Schmelzle, J. S. Brugge *et al.*, *Nat. Methods*, **4**, 855 (2007).
- <sup>6</sup> L. G. Griffith and M. A. Swartz, *Nat. Rev. Mol. Cell Biol.*, **7**, 211 (2006).
- <sup>7</sup> Y. Aizawa, S. C. Owen and M. S. Shoichet, *Prog. Polym. Sci.*, **37**, 645 (2012).
- <sup>8</sup> H. K. Dhiman, A. R. Ray and A. K. Panda, *Biomaterials*, **26**, 979 (2005).

- <sup>9</sup> S. K. Sahoo, A. K. Panda and V. Labhassetwar, *Biomacromolecules*, **6**, 1132 (2005).
- <sup>10</sup> F. Xu and K. J. Burg, *Cytotechnology*, **54**, 135 (2007).
- <sup>11</sup> B. J. Gill and J. L. West, *J. Biomech.*, 2013, doi:10.1016/j.jbiomech.2013.1009.1029.
- <sup>12</sup> O. Hartman, C. Zhang, E. L. Adams, M. C. Farach-Carson, N. J. Petrelli *et al.*, *Biomacromolecules*, **10**, 2019 (2009).
- <sup>13</sup> A. M. Greiner, M. Jäckel, A. C. Scheiwe, D. R. Stamow, T. J. Autenrieth *et al.*, *Biomaterials*, **35**, 611 (2014).
- <sup>14</sup> C. Martínez Ramos, A. Vallés Lluch, J. M. G. Verdugo, J. L. G. Ribelles, J. A. Barcia Albacar *et al.*, *J. Biomed. Mater. Res. A*, **100**, 3276 (2012).
- <sup>15</sup> J. C. Le Huec, T. Schaefferbeke, D. Clement, J. Faber and A. Le Rebeller, *Biomaterials*, **16**, 113 (1995).
- <sup>16</sup> J. M. Taboas, R. D. Maddox, P. H. Krebsbach and S. J. Hollister, *Biomaterials*, **24**, 181 (2003).
- <sup>17</sup> L. S. Wray, K. Tsioris, E. S. Gil, F. G. Omenetto and D. L. Kaplan, *Adv. Funct. Mater.*, **23**, 3404 (2013).
- <sup>18</sup> R. Bagherzadeh, M. Latifi, S. S. Najjar and L. Kong, *J. Biomed. Mater. Res. A*, **101**, 765 (2013).
- <sup>19</sup> K.-W. Lee, S. Wang, M. Dadsetan, M. J. Yaszemski and L. Lu, *Biomacromolecules*, **11**, 682 (2010).
- <sup>20</sup> C. S. Szot, C. F. Buchanan, P. Gatenholm, M. N. Rylander and J. W. Freeman, *Mater. Sci. Eng. C*, **31**, 37 (2011).
- <sup>21</sup> R. A. N. Pertile, S. Moreira, R. M. Gil da Costa, A. Correia, L. Guardao *et al.*, *J. Biomater. Sci. Polym. Ed.*, **23**, 1339 (2012).
- <sup>22</sup> Q. Shi, Y. Li, J. Sun, H. Zhang, L. Chen, B. Chen, H. Yang and Z. Wang, *Biomaterials*, **33**, 6644 (2012).
- <sup>23</sup> N. Petersen and P. Gatenholm, *Appl. Microbiol. Biotechnol.*, **91**, 1277 (2011).
- <sup>24</sup> D. Klemm, F. Kramer, S. Moritz, T. Lindstrom, M. Ankerfors *et al.*, *Angew. Chem. Int. Ed.*, **50**, 5438 (2011).
- <sup>25</sup> C. Gao, Y. Wan, C. Yang, K. Dai, T. Tang *et al.*, *J. Porous Mater.*, **18**, 139 (2011).
- <sup>26</sup> Y. Z. Wan, Y. Huang, C. D. Yuan, S. Raman, Y. Zhu *et al.*, *Mater. Sci. Eng. C*, **27**, 855 (2007).
- <sup>27</sup> Y. Z. Wan, L. Hong, S. R. Jia, Y. Huang, Y. Zhu *et al.*, *Compos. Sci. Tech.*, **66**, 1825 (2006).
- <sup>28</sup> L. Hong, Y. L. Wang, S. R. Jia, Y. Huang, C. Gao *et al.*, *Mater. Lett.*, **60**, 1710 (2006).
- <sup>29</sup> H. Luo, G. Xiong, D. Hu, K. Ren, F. Yao *et al.*, *Mater. Chem. Phys.*, **143**, 373 (2013).
- <sup>30</sup> V. Karageorgiou and D. Kaplan, *Biomaterials*, **26**, 5474 (2005).
- <sup>31</sup> M. Flaibani and N. Elvassore, *Mater. Sci. Eng. C*, **32**, 1632 (2012).
- <sup>32</sup> N. D. Evans, E. Gentleman and J. M. Polak, *Mater. Today*, **9**, 26 (2006).
- <sup>33</sup> H. Sai, K. W. Tan, K. Hur, E. Asenath-Smith, R. Hovden *et al.*, *Science*, **341**, 530 (2013).
- <sup>34</sup> J. Li, Y. Z. Wan, L. F. Li, H. Liang and J. H. Wang, *Mater. Sci. Eng. C*, **29**, 1635 (2009).
- <sup>35</sup> K. M. Chrobak, D. R. Potter and J. Tien, *Microvasc. Res.*, **71**, 185 (2006).